Available online at www.sciencedirect.com
SCIENCE DIRECT®
Carbohydrate Research 339 (2004) 2381–2390
Carbohydrate RESEARCH

MM3 Potential energy surfaces of α-3-linked L-fucobiose and fucotriose and their sulfated counterparts☆

Carlos A. Stortz*

Departamento de Química Orgánica-CIHIDECAR, Facultad de Ciencias Exactas y Naturales, Universidad de Buenos Aires, Ciudad Universitaria, 1428 Buenos Aires, Argentina

Received 4 May 2004; accepted 10 June 2004
Available online 9 September 2004

Abstract—The adiabatic potential energy surfaces (PES) of α-L-Fuc-(1 → 3)-α-L-Fuc and their counterparts disulfated at 2,2′ and 4,4′, and tetrasulfated at 2,2′,4,4′, which are representative of fucoidan structures, were obtained using the MM3 force field, and plotted as contour maps and as 2D graphs representing the energy versus the ψ angle. The surfaces of the corresponding trisaccharides were also obtained and represented by a single 3D contour map for which the energy is plotted against the two ψ glycosidic angles. For the nonsulfated disaccharide, similar populations of two minima occur. A substantial sulfate effect is observed. Whereas sulfation on both of the 2-positions shift the global minimum to positive ψ^H angles, sulfation on both of the 4-positions deepen the well at negative ψ^H values. A similar effect occurred in their galactose counterparts. Sulfation on the 2- and 4-positions carry the additive effect of both groups. The same trend was observed for both linkages present in the trisaccharides, with minor differences. For instance, the 4,4′,4″ trisulfated compound exhibits a trend by which the glycosidic linkage closer to the nonreducing end appears to be highly flexible, with similar energies in both conformers. Raising the dielectric constant on nonsulfated oligosaccharides was found to give a better agreement with experimental determinations.

Keywords: Trisaccharides; Fucoidans; Fucose; Conformational analysis; Molecular mechanics; MM3; Ramachandran map; Potential energy surfaces

1. Introduction

The functional and biological properties of carbohydrates depend on their conformational features. This spawned a genuine interest in the determination of their three-dimensional structures by both experimental and theoretical methods. Modeling of disaccharides is usually accompanied by the generation of Ramachandran-like 3D contour plots that relate the potential energy of the molecules and the glycosidic angles ϕ and ψ.[2–4] In the past 15 years, these maps have been constructed by flexible-residue analysis[5–8] especially with the aid of the MM3 force field,[9,10] which is considered to be reasonably reliable for most carbohydrates. As the ϕ glycosidic angle usually takes a more or less fixed value (at least with MM3) it can be allowed to relax, and the energy can be related directly to ψ.[11] Therefore, we were able to present the potential energy surfaces (PES) of trisaccharides as contour maps in which the energy is plotted as a function of both ψ glycosidic angles, finding very little influence of one linkage over the other in most cases,[1,12,13] but a strong influence in other products where a hydrogen bond between the first and the third monosaccharide units alters the shape of the PES expected from placing both disaccharide maps together.[1,13]

Fucoidans are an important group of polysaccharides obtained mostly from brown seaweeds,[14] but also from echinoderms.[15,16] It has been reported that they carry several biological activities, especially antiviral.[14] In spite of the many attempts to determine their fine structural features, only a few examples of regularity were found.[17] However, activity among fucoidans clearly depends on the shape and charge features of

☆ MM3 Potential energy surfaces of trisaccharides. Part 4. For Part 3, see Ref. 1.

* Tel./fax: +54-11-4576-3346; e-mail: stortz@qo.fcen.uba.ar

0008-6215/$ - see front matter © 2004 Elsevier Ltd. All rights reserved.
doi:10.1016/j.carres.2004.06.024

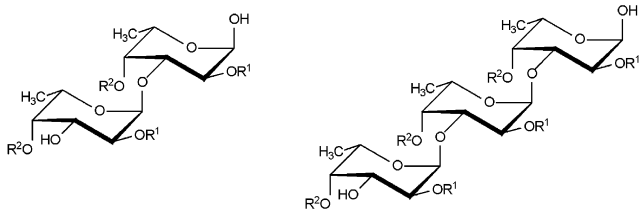

1d	$R^1 = R^2 = H$	**1t**	$R^1 = R^2 = H$
2d	$R^1 = SO_3^-$, $R^2 = H$	**2t**	$R^1 = SO_3^-$, $R^2 = H$
3d	$R^1 = H$, $R^2 = SO_3^-$	**3t**	$R^1 = H$, $R^2 = SO_3^-$
4d	$R^1 = R^2 = SO_3^-$	**4t**	$R^1 = R^2 = SO_3^-$

Figure 1. The di- and trisaccharides studied in this work.

some fragments.[18] The group of Nifantiev has started a series of papers reporting the synthesis and conformational studies of fucoidan fragments.[18] They have presented the first PES analysis for such fragments and compare them with experimentally determined features.[19,20]

In connection with our work on bioactive fucoidans,[14] herein is presented a systematic analysis of the MM3 potential energy surfaces of the disaccharide α-L-Fuc-(1 → 3)-α-L-Fuc, the trisaccharide α-L-Fuc-(1 → 3)-α-L-Fuc-(1 → 3)-α-L-Fuc, and their derivatives sulfated at the 2- and 4-positions (Fig. 1).

2. Methods

The molecular mechanics program MM3(92) (QCPE, Indiana University, USA), developed by Allinger and co-workers, was used,[9,10] but the MM3 routines were modified as suggested[21] by changing the maximum atomic movement from 0.25 to 0.10 Å. MM3 parameters for the sulfate group were taken from Lamba et al.,[22] and a dielectric constant of 3.0 was used. In that model, the charge on the sulfate groups is emulated by S–O bond dipoles, with no cations added. A dielectric constant of 80 was also used in some cases (see Section 3). Minimizations were carried out by the block diagonal Newton–Raphson procedure for grid points and using the full-matrix procedure for minima, and were terminated when the energy converged to a value lower than 2 cal/mol. The dihedrals ϕ and ψ for the disaccharides are defined by atoms O-5′–C-1′–O-1′–C-3 and C-1′–O-1′–C-3–C-4, respectively, while ϕ^H and ψ^H are defined by atoms H-1′–C-1′–O-1′–C-3 and C-1′–O-1′–C-3–H-3, respectively. For the trisaccharides, the constituting monosaccharides are numbered starting from the reducing end. The dihedral angles $\phi_{2\rightarrow1}$ and $\psi_{2\rightarrow1}$ and their hydrogen-related counterparts are defined exactly as those of the disaccharides, whereas the equivalent dihedrals for the 3 → 2 linkage follow the same conventions, but nonprimed atoms should be primed, while those primed should be double-primed.

The orientation of the hydroxyl hydrogen atoms is indicated by χ_n, defined by the atoms H-*n*–C-*n*–O-*n*–H(O)-*n*, singly- or double-primed when necessary. Their values are described by a one-letter code:[23] **S** for angles between −30° and +30°, **g** for 30–80°, **T** for angles with absolute value larger than 150°, and **G** for angles between −30° and −80°. All starting points had their chairs in the most stable, $^1C_4$ conformation.

In order to proceed with NOE theoretical calculations, the average matrix of H–H distances was obtained from the statistical population of the minima as shown by Imberty et al.[24] Once this matrix was obtained, the NOEs were computed by an iterative procedure[25] and expressed as increases in ^{1}H NMR peak intensity when irradiating the anomeric proton, relative to the NOE on its neighboring proton H-2.

2.1. Generation of disaccharide potential energy surfaces

To generate the maps, ca. 10–25 conformers in different ψ regions were chosen for each disaccharide, with varied orientations of the secondary hydroxyl (or sulfate) groups, and taken as starting points. These starting conformers were chosen with the aid of the study of a similar disaccharide where D-galactose replaced the L-fucose (and with a inverted configuration at the reducing end),[11,26] and also using iterative procedures.[4] The 2D plots were obtained as described:[11] beginning with all the starting conformers, minimizations with a restrained ψ in 10° intervals (the remaining variables allowed to relax) were carried out using both the dihedral drivers 2 (sequential minimization) and 4 (minimization from the starting point). The energy for each ψ point was the lowest of all the calculations, thus giving rise to a 2D conformational adiabatic plot as a function of the ψ angle. A similar procedure,[27] but extending on a 20° grid at both the ϕ and ψ angles, was used to produce the adiabatic contour map. For the studies at $\varepsilon = 80$, all 729 combinations of the three-fold staggered orientations for the six rotatable exocyclic groups were generated in each minimum-energy region, and those with lower energy (less than 1 kcal/mol above the global minimum) were left to generate the trisaccharide minima.

2.2. Generation of the trisaccharide minima

The following general procedure was used:[1,12] Different starting orientations of the hydroxyl (or sulfate) groups of the trisaccharides were tested, using as data the conformers that yielded at least one low-energy grid point in the disaccharide maps (or, for the studies at $\varepsilon = 80$, those of lower energy). In this way, many different combinations of orientations of the exocyclic groups were tested (48 for **1t** at $\varepsilon = 80$, 36 for **1t** at $\varepsilon = 3$ and 4,4′,4″-trisulfated **3t**, 3 for the 2,2′,2″-trisulfated **2t**, 4 for the hexasulfated **4t**). In an automated fashion, unrestrained MM3

full-matrix calculations were carried out for points starting at each of those orientations, i.e., at each of the three different combination of the ϕ, ψ angles (in either of both linkages) that gave rise to a minimum in the disaccharide maps. In the final output for each minimum, only those orientations with an energy up to 1 kcal/mol above the lowest in that $\psi_{2\rightarrow1}$, $\psi_{3\rightarrow2}$ region were left. The conformers produced were used to generate the maps (see below). During this generation, it was determined that new minima in unexpected regions appeared for **4t**. These minima were identified and characterized and added as new starting points for the generation of the map. For **1t**, a total of 82 conformers were found, corresponding to 21 unique orientations of the exocyclic groups, while for **2t** only 18 different conformers were encountered, corresponding to two different orientations of the hydroxyl groups. For **3t**, 54 total conformers corresponded to 24 unique orientations of the exocyclic groups, whereas for **4t**, 33 total conformers carried 4 different orientations of the hydroxyl groups.

2.3. Generation of trisaccharide maps

The maps were generated following the general procedures described for di- and trisaccharides.[1,12] As explained previously,[1] as the minimum-energy ϕ angles showed considerable variations in different regions of some maps, the MM3 driver 2 (sequential) was used starting from each conformer in four different directions, in order to search as much as possible for low-energy grid points, as the use of this driver in only one direction might have lead to the propagation of inelastic deformations that would have affected[4] the adiabaticity of the maps. Driver 4 was also used, once for each unique orientation of exocyclic angles when the ϕ values did not differ largely. Otherwise, driver 4 was used from more than one exocyclic combination. In all cases, the angles $\psi_{2\rightarrow1}$ and $\psi_{3\rightarrow2}$ were fully varied using a 20° grid. At each point, energies were calculated after minimization with restraints for these two angles but allowing the other variables (including both ϕ angles) to relax. The conformational adiabatic maps were produced by recording the lowest energy values for each ψ, ψ combination. In order to recalculate the surface in the region where the main minima appear (both ψ from 170° to 310°), the starting points that yielded low-energy grid points in this region were submitted to calculations using the same procedure described above, but with a 5° grid.

2.4. Flexibility measurements

The absolute flexibility gives an indication of the ease at which the low-energy conformers overcome barriers to their conformational interconversions. This parameter was calculated for di- and trisaccharides as described previously[1,12,28] and extended to each glycosidic linkage. For this purpose, the absolute flexibility for each of the paths (when they exist) involving a neat variation of the ψ angle corresponding to this linkage was calculated independently. The partition functions (total and partial on each ψ torsional angle) were calculated as described previously.[1,12]

3. Results

The compounds under study and their acronyms appear in Figure 1. The MM3 adiabatic potential energy surfaces for **1d**–**4d** (at $\varepsilon = 3$), depicted as energy plots related to the glycosidic angle ψ[11] (i.e., with the ϕ angles relaxed to their minimum-energy position in the main trough) are shown in Figure 2, while the corresponding 3D contour maps are shown in Figure 3. Table 1 shows the geometrical and energy characteristics of the lower-energy minima in each region, including those calculated for **1d** at $\varepsilon = 80$. At a dielectric constant of 3, the nonsulfated compound **1d** exhibits a typical three-minima behavior, with very small energy differences between those labeled as **A** and **B**. Both in the studies of this compound at $\varepsilon = 80$, and of those of the compound sulfated at C-2 (**2d**) at $\varepsilon = 3$, **B** becomes the global minimum, whereas for that sulfated at C-4 (**3d**), **A** is the global minimum. An approximately additive effect of both sulfate groups occurs in compound **4d**, leading to a **B** global minimum, but less deep than in **2d**.

The MM3 PES ($\varepsilon = 3$) of the trisaccharides **1t**–**4t** determined as a contour map relating the energy to both ψ glycosidic angles is shown in Figure 4, whereas the equivalent plots obtained by recalculation in the region **A**–**B** of low energy (both ψ angles from 170° to 310°) are shown in Figure 5. The geometrical and energy data on the main minima obtained in each region for compound

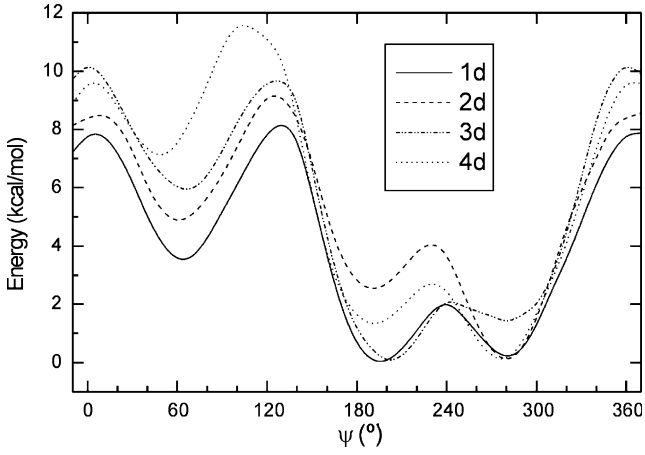

Figure 2. MM3(92) relaxed surface (2D plot) for disaccharides **1d**–**4d** at $\varepsilon = 3$.

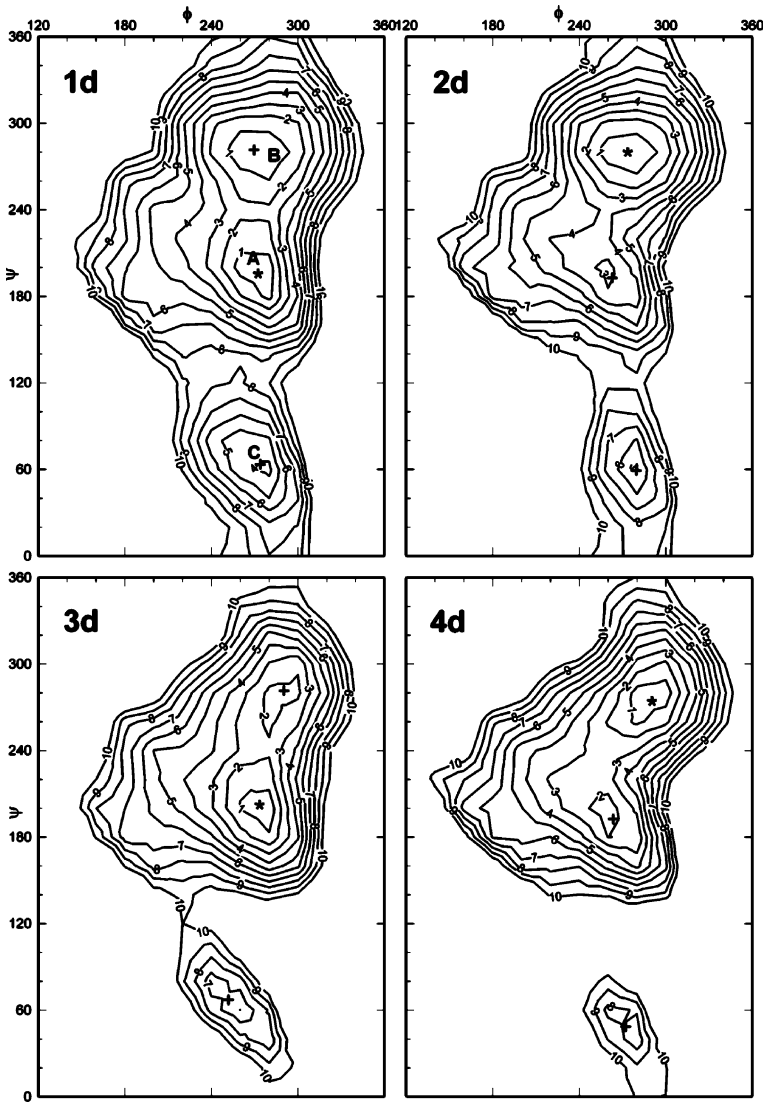

Figure 3. MM3(92) adiabatic conformational maps (3D) of disaccharides **1d**–**4d** at $\varepsilon = 3$. Isoenergy contour lines are graduated in 1 kcal/mol increments above the global minimum. The symbols indicate: (*) MM3 global minima; (+) MM3 local minima.

1t at both $\varepsilon = 3$ and $\varepsilon = 80$ are shown in Table 2, whereas these data for the other three trisaccharides are shown in Table 3. The minima are named by a two-letter code according to the minimum energy region (**A**, **B**, or **C**) of the 3 → 2 linkage (first letter) and the 2 → 1 linkage (second letter).[1] Table 4 shows the flexibility measurements carried out using the data obtained for the di- and trisaccharides under study. Table 5 shows the hydrogen-bond arrangements expected to occur in the polysaccharides with the repeating structure of **1**–**4**, deduced from those occurring at the minimum energy conformations of the di- and trisaccharides under study. Table 6 shows the calculated NOE effects on the compounds under study when irradiating the anomeric proton, considering the population of each conformer.

4. Discussion

4.1. Potential energy surfaces of the nonsulfated disaccharide and trisaccharide

Many studies were devoted to flexible-residue molecular modeling of different disaccharides,[2–8] especially after the appearance of MM3,[9,10] a force field with good parameterization for carbohydrates. Recently, those studies were extended to different trisaccharides,[1,12,13] in an attempt to achieve a better knowledge of the conformational features of polysaccharides. For α-(1 → 3)-linked fucobiose **1d**, present calculations show a typical three-minima pattern (Figs. 2 and 3, Table 1), with very little energy difference between the minima labeled as **A** and **B** (Table 1). These results are very similar to those

Table 1. Torsion angles (°), relative steric energies (kcal/mol), and exocyclic angles for the minimum-energy conformations obtained for the disaccharides **1d**–**4d** using the MM3 force field; selected data for the main transition states (TS) is also included

	ϕ, ψ	ϕ^H, ψ^H	E_{rel}	Exocyclic torsion angles[a]	
				$\chi_{2'}\chi_{3'}\chi_{4'}$	$\chi_1\chi_2\chi_4$
1d (ε = 3)					
A	273, 195	33, −48	0.00	gGG	gGG
B	270, 282	30, 44	0.14	GgG	GGG
C	272, 64	32, −179	3.44	GgG	GGG
TS **A** ↔ **B**	268, 241	27, 1	2.10		
1d (ε = 80)					
A	269, 194	30, −49	1.24	gGG	ggG
B	279, 277	38, 39	0.00	gGG	gGG
C	272, 62	33, 179	4.79	gGS	GgG
2d					
A	265, 190	25, −53	2.46	SGG	GgG
B	274, 280	34, 42	0.00	SGG	GSG
C	279, 60	40, 177	4.79	SGG	GSG
TS **A** ↔ **B**	254, 232	14, −10	4.10		
3d					
A	273, 203	34, −40	0.00	TGS	GGS
B	290, 282	50, 44	1.34	gGS	GGS
C	252, 67	12, −176	5.86	GTS	GGS
TS **A** ↔ **B**	276, 224	37, −18	2.38		
4d					
A	265, 191	26, −52	1.28	SGS	GgS
B	291, 277	51, 39	0.00	SGS	GSS
C	272, 49	33, 167	7.02	SGS	GgS
TS **A** ↔ **B**	253, 235	13, −7	2.83		

[a] For nomenclature, see Section 2.

observed for α-(1 → 3)-linked galactobiose,[4,26] indicating that the hydroxymethyl groups have little influence over the conformational features of the glycosidic linkage of these disaccharides. As expected, the conformational map (and the sign of the angles) of fucobiose appears inverted, as they correspond to the L–L disaccharide, whereas the previous ones[4,26] corresponded to a D–D-galactobiose. When the calculations were repeated at a dielectric constant of 80, where the electrostatic and hydrogen bond interactions are almost suppressed, minimum **B** appears stabilized with respect to **A** (Table 1), as occurred with the galactobiose counterpart.[4] This result is probably due to the fact that at a lower dielectric constant, minimum **A** appears stabilized by a hydrogen bond between H(O)-2 and O-5′ (Table 5), whereas at a high dielectric constant this hydrogen bond is weakened or precluded, thus favoring relatively minimum **B**. These results are qualitatively similar to those obtained by Gerbst and co-workers[19,20] using a similar (but not identical) method of calculation at high dielectric constants. However, although no energies of each minimum are supplied by the authors,[19] the reported Boltzmann population ratio (1:1.6) suggests that the energy difference between minima **A** and **B** is lower in their work. Modeling of the corresponding trisaccharide **1t** leads to four main minima (**AA**, **AB**, **BA**, and **BB**) with very similar energies (Table 2, Figs. 4 and 5). This map resembles closely that observed for cellotriose.[12] When the calculations were repeated at ε = 80, both glycosidic angles prefer the **B** orientation as occurred with the disaccharide, leading to **BB** as the most populated minimum (81%). A similar result (82% population) was obtained by Gerbst et al.[20] by construction of a stepwise map for each glycosidic linkage.

4.2. Potential energy surfaces of sulfated disaccharides and trisaccharides

Introduction of a sulfate group on both C-2 of the disaccharide leads to the compound **2d**. The conformational surface was calculated only at ε = 3, as the parameters for emulating the sulfate group in MM3 were devised for this dielectric constant.[22] The PES appears similar to that of **1d**, but conformation **B** (with H-1′ closer to H-4 than to H-3) becomes highly favored (Table 1, Figs. 2 and 3). This can be explained in terms of a hydrogen bond lost by sulfation in conformer **A** and another one gained by sulfation in conformer **B** (Table 5). The surface of trisaccharide **2t** (Table 3, Figs. 4 and 5) shows the behavior expected from that of the disaccharide. Minimum **BB** is the global one, being the remaining minima with a population lower than 5%. The introduction of a sulfate group on C-4 leads to the opposite trend: the PES of **3d** shows conformer **A** as the global minimum. Gerbst et al. obtained a similar qualitative result,[19] despite their use of a different dielectric constant. Their work, however, suggests a lower difference of energy between the two conformers.[19] When the PES of the corresponding trisaccharide (**3t**) is analyzed, it is shown that for the linkage closer to the reducing end, the **A** conformation is still preferred, but for the other linkage there are regions of the map where the **B** conformation is slightly more favorable (Table 3, Fig. 5). Thus, the conformation **BA** appears to be a global minimum (61% population), closely followed by minimum **AA** (35% population). It is noteworthy, however, that the **B** conformer in **BA** has a ψ angle of lower magnitude than those usual in **B** conformers (Table 3), leading to a H-1″ at a similar distance from H-3′ and H-4′. The calculations of Gerbst et al.[20] (ε = 81, Tinker MM3) indicate a 70% population of conformer **AA**, 18% of **BA**, and 12% of **AB**.

For the disaccharide sulfated at both the C-2 and C-4 positions (**4d**), the additive effect of sulfation shown in **2d** and **3d** occurs. Minimum **B** appears as the global one, but not as deep as happens for the 2-sulfated compound **2d**, as the effect of 4-sulfate partially offsets its predominance. For the trisaccharide **4t** (Table 3, Figs.

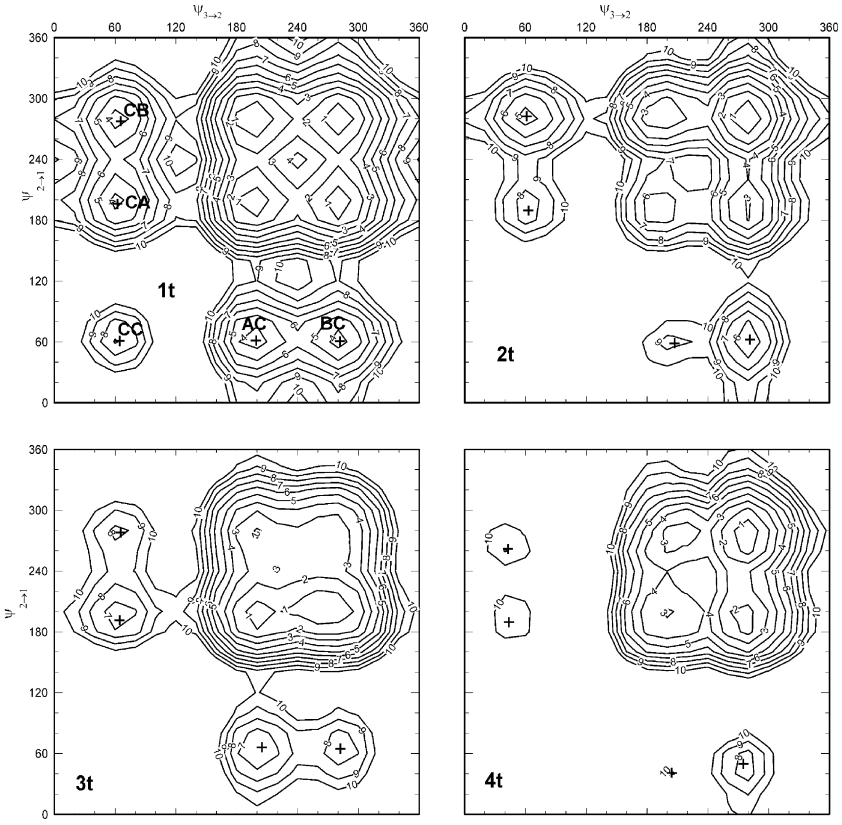

Figure 4. MM3(92) adiabatic conformational maps (energy vs $\psi_{3\rightarrow 2}$, $\psi_{2\rightarrow 1}$) of trisaccharides **1t**–**4t** at $\varepsilon = 3$. Isoenergy contour lines are graduated in 1 kcal/mol increments above the global minimum. The symbol (+) indicates some of the MM3 local minima.

4 and 5), **BB** appears as the global minimum, leading to a shape similar to that observed for **2t** (Fig. 5). However, the energies of the remaining minima (especially that of **BA**) are much lower.

4.3. Comparison with experimental data

Among the experimental data used to assess the validity of the calculation results for carbohydrates, probably the most important is the measurement of the nuclear Overhauser effect (NOE). In order to measure the conformational features of oligosaccharides around the glycosidic bond, the determination of NOE values when irradiating the anomeric proton H-1′ perceived by the closer protons of the 'aglycon' is especially important. For 3-linked disaccharides, the most important effect to measure is that on H-3 and H-4. NOE values can be measured in either steady-state or transient mode.[19] By either of these techniques, the experimental NOE values were measured by Gerbst and co-workers[19,20] for the *n*-propyl glycosides of **1d**, **1t**, **3d**, and **3t**. NOE values give an idea of the proximity of the protons. Thus, conformation **A** (H-1′ closer to H-3 than to H-4) leads to a high NOE on H-3 and a negligible one on H-4. On the other hand, conformation **B** (H-1′ closer to H-4) leads to a considerable NOE on H-3, but a much higher one on H-4. The expected NOEs for each conformer can be theoretically calculated, and those expected for real compounds containing different conformers can also be calculated with proper averaging (see Section 2). The calculated and experimental NOEs (expressed as a ratio between that on H-3 and that on H-4) appear in Table 6. For compound **1d** the experimental value[19] (0.92) indicates a predominance of the **B** conformer, but a substantial proportion of **A** conformer. Our results at $\varepsilon = 3$ (1.50) overestimate the proportion of the **A** conformer, while those at $\varepsilon = 80$ (0.67) underestimate it. The results of Gerbst and co-workers[19,20] are similar to ours at $\varepsilon = 80$, but they report that they have improved the calculations by taking into account not just the main minima, but also the low-energy regions around them. When instead of the disaccharide, the trisaccharide **1t** is being studied, the proportion of **B** conformers appear to increase, thus decreasing the expressed ratio. This decrement occurs for the calculation at $\varepsilon = 80$ (from 1.5 to 1.2–1.4), at $\varepsilon = 3$ (from 0.67 to 0.49–0.52), as well as for the experimental value (from 0.92 to 0.70, Table 6). This increase in the proportion of **B** conformers was already shown to appear in previous work.[20] In a previous paper,[4] we have already shown a better agreement with experimental NOE values when working at $\varepsilon = 80$. When sulfate groups are introduced at C-4 (**3d**

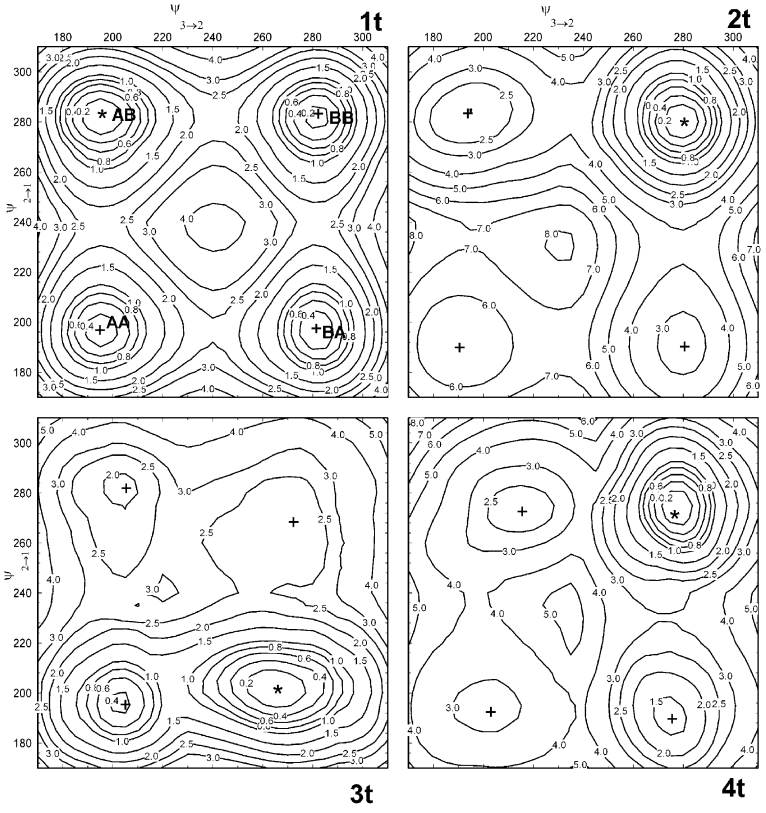

Figure 5. MM3(92) adiabatic conformational maps (energy vs $\psi_{3\rightarrow 2}$, $\psi_{2\rightarrow 1}$) of trisaccharides **1t**–**4t** at $\varepsilon = 3$, recalculated in the low-energy region. Isoenergy contour lines are graduated in 0.2 kcal/mol increments above the global minimum, up to 1 kcal/mol, and then in 0.5 kcal/mol increments. The symbols indicate: (*) MM3 global minima; (+) MM3 local minima.

Table 2. Torsion angles (°), relative steric energies (kcal/mol), and exocyclic angles for the main minimum-energy conformations obtained for compound **1t** at two different dielectric constants; selected data for the main transition states (TS) at $\varepsilon = 3$ is also included

	$\phi_{3\rightarrow 2}$, $\psi_{3\rightarrow 2}$	(ϕ^H, ψ^H)	$\phi_{2\rightarrow 1}$, $\psi_{2\rightarrow 1}$	(ϕ^H, ψ^H)	E_{rel}	Exocyclic torsion angles[a]		
						$\chi_{2''}\chi_{3''}\chi_{4''}$	$\chi_{2'}\chi_{4'}$	$\chi_1\chi_2\chi_4$
1t ($\varepsilon = 3$)								
AA	271, 195	31, −48	272, 197	32, −46	0.28	gGG	GG	GGG
AB	272, 195	32, −47	267, 283	26, 45	0.00	gGG	GG	GGG
AC	272, 195	32, −47	271, 64	31, −179	3.35	gGG	GG	GGG
BA	272, 282	31, 44	272, 196	32, −46	0.23	GgG	GG	GGG
BB	272, 282	32, 44	270, 282	30, 44	0.10	GgG	GG	GGG
BC	270, 282	30, 44	272, 64	32, −179	3.46	GgG	GG	GGG
CA	271, 64	32, −179	272, 197	32, −46	3.59	GgG	GG	GGG
CB	272, 64	32, −179	271, 282	29, 44	3.42	GgG	GG	GGG
CC	271, 64	32, −179	272, 64	32, −179	6.78	GgG	GG	GGG
TS **AA** ↔ **AB**	271, 195	31, −47	267, 241	27, 1	2.27			
TS **AA** ↔ **BA**	267, 241	27, 1	272, 197	31, −46	2.38			
TS **AB** ↔ **BB**	268, 241	27, 1	268, 282	27, 44	2.19			
TS **BA** ↔ **BB**	272, 282	32, 43	267, 241	27, 1	2.26			
1t ($\varepsilon = 80$)								
AA	269, 193	29, −50	269, 193	29, −50	2.63	gGG	gG	ggG
AB	269, 193	29, −50	280, 280	40, 41	1.32	gGG	gG	gGG
AC	269, 192	29, −50	273, 59	33, 176	6.15	gGG	gG	gGS
BA	282, 280	42, 41	269, 193	30, −50	1.31	gGG	GG	ggG
BB	282, 280	41, 41	281, 280	40, 42	0.00	gGG	GG	gGG
BC	282, 280	41, 41	272, 60	33, 177	4.80	gGG	GG	gGS
CA	272, 60	33, 177	269, 192	29, −50	6.22	GgG	GS	ggG
CB	272, 60	33, 177	281, 280	40, 41	4.87	GgG	GS	gGG
CC	272, 60	33, 177	272, 60	33, 177	9.68	GgG	GS	gGS

[a] For nomenclature, see Section 2.

Table 3. Torsion angles (°), relative steric energies (kcal/mol), and exocyclic angles for the main minimum-energy conformations obtained for compounds **2t**–**4t** using the MM3 force field (minima with energies 10 kcal/mol above the global minimum are not included); selected data for the main transition states (TS) is also included

	$\phi_{3\to2}$, $\psi_{3\to2}$	(ϕ^H, ψ^H)	$\phi_{2\to1}$, $\psi_{2\to1}$	(ϕ^H, ψ^H)	E_{rel}	Exocyclic torsion angles[a]		
						$\chi_{2''}\chi_{3''}\chi_{4''}$	$\chi_{2'}\chi_{4'}$	$\chi_1\chi_2\chi_4$
2t								
AA	262, 191	22, −52	265, 191	25, −52	5.27	SGG	gG	GgG
AB	256, 195	16, −48	290, 283	50, 45	1.97	SGG	gG	GSG
AC	240, 205	−1, −37	277, 59	38, 176	8.53	SGG	SG	GgG
BA	275, 280	35, 41	265, 191	25, −52	2.62	SGG	SG	GgG
BB	276, 279	36, 41	276, 281	36, 42	0.00	SGG	SG	GSG
BC	274, 280	34, 42	276, 62	37, 179	5.09	SGG	SG	GgG
CA	279, 61	40, 178	265, 191	24, −52	7.27	SGG	SG	GgG
CB	278, 59	39, 176	289, 283	48, 45	4.45	SGG	SG	GgG
TS **AA** ↔ **AB**	253, 196	13, −47	256, 235	16, −6	6.63			
TS **AA** ↔ **BA**	255, 231	15, −11	264, 191	24, −52	6.61			
TS **AB** ↔ **BB**	256, 235	16, −6	289, 285	48, 46	3.59			
TS **BA** ↔ **BB**	276, 279	36, 41	253, 231	13, −10	4.11			
3t								
AA	272, 204	32, −39	271, 196	31, −47	0.33	TGS	GS	GGS
AB	272, 203	32, −39	288, 282	47, 44	1.84	TGS	GS	GGS
AC	272, 203	33, −40	253, 66	13, −177	5.96	TGS	GS	GGS
BA	284, 265	44, 25	273, 202	34, −41	0.00	TGS	TS	GGS
BB	289, 272	49, 33	285, 266	45, 27	2.00	TGS	TS	gTS
BC	291, 281	50, 43	251, 67	11, −176	7.16	gGS	GS	GGS
CA	253, 66	13, −177	272, 196	32, −47	6.27	GTS	GS	GGS
CB	253, 66	13, −177	288, 281	48, 43	7.57	GTS	GS	GGS
TS **AA** ↔ **AB**	270, 197	30, −46	265, 244	24, 4	2.82			
4t								
AA	243, 202	3, −40	265, 193	25, −50	2.76	SGS	SS	GgS
AB	230, 215	−12, −27	288, 273	48, 35	2.18	SGS	SS	GSS
AC	243, 204	3, −39	271, 47	32, 165	9.65	SGS	SS	GgS
BA	289, 275	49, 36	266, 190	26, −53	1.32	SGS	SS	GgS
BB	294, 277	54, 39	288, 274	49, 36	0.00	SGS	SS	GSS
BC	293, 276	53, 38	269, 49	29, 167	7.14	SGS	SS	GgS
CA	275, 48	35, 166	266, 191	25, −52	8.85	SGS	gS	GgS
CB	279, 44	40, 163	282, 265	41, 25	8.78	SGS	SS	GSS
TS **AA** ↔ **AB**	247, 197	6, −45	255, 239	14, −2	3.93			
TS **AA** ↔ **BA**	254, 235	14, −6	265, 193	25, −51	4.15			
TS **BA** ↔ **BB**	282, 268	42, 29	254, 231	13, −11	2.98			

[a] For nomenclature, see Section 2.

Table 4. Corrected partition functions q and absolute flexibilities Φ calculated for the compounds under study

		q_ψ (deg)	$q_{\phi,\psi}$ (deg^2)	$\Phi_{\phi,\psi}$ (×10^4)	Φ_ψ (×10^4)	$\Phi_{\phi,\psi}/\Phi_\psi$
1d		52	1390	19	35	0.54
2d		23	760	0.9	1.3	0.71
3d		31	600	7	12	0.58
4d		28	640	9	10	0.92
	$q_{\psi,\psi}$ (deg^2)	q_ψ (deg)	$\Phi_{\phi,\psi,\phi,\psi}$, (×10^4)	$\Phi_{\psi,\psi}$ (×10^4)	Φ_ψ (×10^4)	$\Phi_{\phi,\psi,\phi,\psi}/\Phi_{\psi,\psi}$
1t	2270	$q_{\psi_{3\to2}} = 47$[a] $q_{\psi_{2\to1}} = 43$[a]	14	26	$\Phi_{\psi_{3\to2}} = 31$ $\Phi_{\psi_{2\to1}} = 28$	0.55
2t	656	$q_{\psi_{3\to2}} = 24$[a] $q_{\psi_{2\to1}} = 23$[a]	1.7	2.2	$\Phi_{\psi_{3\to2}} = 2.8$ $\Phi_{\psi_{2\to1}} = 1.3$	0.80
3t	1624	$q_{\psi_{3\to2}} = 56$[a] $q_{\psi_{2\to1}} = 28$[a]	1.4	2.4	 $\Phi_{\psi_{2\to1}} = 7.3$	0.59
4t	675	$q_{\psi_{3\to2}} = 22$[a] $q_{\psi_{2\to1}} = 27$[a]	4.2	4.6	$\Phi_{\psi_{3\to2}} = 1.0$ $\Phi_{\psi_{2\to1}} = 9.1$	0.92

[a] Estimated from the 3D map (see Section 2).

Table 5. Hydrogen bond arrangements expected to occur in the polysaccharides with the substitution patterns of **1**, **2**, **3**, and **4**[a]

Hydrogen bond	Compound	Minima
H(O)-2–O-5′	**1** and **3**	**A**
H(O)-4–O-5′	**1** and **2**	**C**
H(O)-4–O(S)-2′	**2**	**B**
H(O)-2′–O(S)-4	**3**	**A**, **B**
H(O)-2–O-2′	**3**	**C**

[a] The data is obtained from the hydrogen bonds with $E_{HB} > 0.6$ kcal/mol observed for the four trisaccharides under study at $\varepsilon = 3$.

Table 6. Calculated relative NOE values for the di- and trisaccharides under study; the experimental data for some compounds is included

	NOE on H-3/NOE on H-4[a]	NOE on H-3′/NOE on H-4′[b]
1d ($\varepsilon = 3$)	1.5	
1d ($\varepsilon = 80$)	0.67	
2d	0.53	
3d	30	
4d	0.45	
1t ($\varepsilon = 3$)	1.2	1.4
1t ($\varepsilon = 80$)	0.52	0.49
2t	0.49	0.53
3t	25	2.2
4t	0.59	0.35
Experimental[c]		
1d	0.92	
3d	2.0	
1t	0.70	0.70
3t	1.7	1.7

[a] When irradiating H-1′.
[b] When irradiating H-1″.
[c] From Refs. 19 and 20.

and **3t**), the **A** conformations become more important. Furthermore, the calculated NOE on H-4 becomes negligible, thus leading to a very high theoretical NOE ratio (Table 6). The experimental values reflect this trend but at a much lower pace: for **3d**, the expected NOE ratio is 2, and for both linkages of **3t** is 1.7. This indicates that either the **A** conformers have a geometry partly shifted from that calculated, or that the proportion of **B** conformers is higher than expected. The last possibility appears supported by our calculations for **3t**, for which a **BA** conformer is slightly preferred over an **AA** one, leading to a calculated NOE ratio on the glycosidic linkage nearer to the nonreducing end (2.2) very close to the experimental value (1.7). Gerbst et al. have found a clear predominance of **AA** conformers.[20] However, they claim that a good correlation with experimental values was encountered when one of the sulfate groups was left protonated, i.e., not as the free anion.[20] At the high dielectric constant used, this effect should be based on steric grounds, as no electrostatic or hydrogen-bonding effect is expected to appear at $\varepsilon = 81$. It is worth noting that our calculations with sulfated compounds might not exactly imitate aqueous solutions, as the parameters introduced by Lamba et al.[22] mostly attempted to emulate the crystal state.

Another experimental value that reflects the same trend is the ^{13}C NMR chemical shift of the anomeric carbon atom. A predominance of the **A** conformer leads to downfield displacements (for its shorter H-1–H-3 distance), while a higher population of **B** conformers leads to upfield displacements.[26] This trend was shown to occur with some of the current compounds. The anomeric carbons of the glycosidically linked moieties in **1d** and **1t** (**B** conformation is predominant) show a chemical shift of 96.4–97.1 ppm,[19,20] whereas in **3d** and **3t**, with predominant **A** conformation, the chemical shifts of the anomeric carbons are displaced to 98.7–99.5 ppm.[19,20] Similarly, 2-sulfated carrageenans show a marked upfield displacement with respect to those 4-sulfated, in agreement with present and previous calculations.[26] Only one crystal structure was reported[29] with a configuration similar to that of **1d**. It corresponds to a peracetylated D-galactosamine disaccharide linked α-(1 → 3). Its glycosidic angles are in our **B** region, the one favored at higher dielectric constants.

4.4. Flexibility measurements

The flexibility observed in disaccharide **1d** is reduced by sulfation (Table 4). The decrease is higher when the equatorial hydroxyl group on C-2 is sulfated than when the axial one on C-4 is sulfated, as expected.[30,31] However, when both the groups on C-2 and C-4 are sulfated, the decrease in flexibility is lowered (Table 4). This may be partly due to a deformation in the ϕ angles to cope with the steric hindering. This deformation does not occur as much in the minima (Table 1) as in the rest of the map, as shown by the high $\Phi_{\phi,\psi}/\Phi_{\psi}$ ratios, which are indicative of a high diversity in ϕ values. A similar trend is observed for the trisaccharides (Table 4). When comparing **1d** and **1t**, the $q_{\psi,\psi}$ for **1t** is lower than the q_{ψ} for **1d**, thus indicating a decrease of the flexibilities of the individual linkages of the trisaccharide with respect to that of the disaccharide, probably due to the presence of cooperative interactions.[12] The other parameter that confirms this decreased flexibility is an estimation of the partition function values for each individual linkage (Table 4). Our results show that the 2 → 1 linkage (closer to the reducing end) appears to be less flexible than the 3 → 2 linkage, as occurred with other trisaccharides.[12] The same effect is shown to occur by measuring absolute flexibilities (Φ_{ψ}). A similar effect was observed when comparing the highly sulfated compounds **4d** and **4t**. However, in this case, the 2 → 1 linkage appears to be more flexible than the 3 → 2 linkage. For compounds **2d/2t**, no decrease in the flexibility from the di- to the trisaccharide was shown to occur. Furthermore, a slight increase appears to occur on the linkage closer

to the nonreducing end. It was already shown that 4-sulfation leads to an unexpected global minimum in the trisaccharide (see above). This fact reflects on the flexibilities. Whereas the flexibility of the $2 \rightarrow 1$ linkage of **3t** is diminished slightly with respect to that of **3d**, the flexibility of the $3 \rightarrow 2$ linkage appears increased (at least by the use of the partition function, as the absolute flexibility could not be calculated) as a consequence of the lowering in energy of the **B** minimum (Table 3), giving rise to a large low-energy **A**–**B** region in the map (Fig. 5).

This work shows once more the advantages of fully relaxed calculations and mapping of trisaccharides by the way of 3D contours in comparison with those of the single disaccharides. The advent of better functional forms or variations in the parameterization in the future may lead to a better coincidence with experimental ones by using the same approach.

Acknowledgements

The author is a Research Member of the National Research Council of Argentina (CONICET). This work was supported by a grant from UBA (X-087). Dr. A. S. Cerezo is acknowledged for helpful discussions.

References

1. Stortz, C. A.; Cerezo, A. S. *Carbohydr. Res.* **2003**, *338*, 1679–1689.
2. French, A. D.; Brady, J. W. *ACS Symp. Ser.* **1990**, *430*, 1–19.
3. Tran, V.; Buléon, A.; Imberty, A.; Pérez, S. *Biopolymers* **1989**, *28*, 679–690.
4. Stortz, C. A. *Carbohydr. Res.* **1999**, *322*, 77–86.
5. Dowd, M. K.; Zeng, J.; French, A. D.; Reilly, P. J. *Carbohydr. Res.* **1992**, *230*, 223–244.
6. Dowd, M. K.; French, A. D.; Reilly, P. J. *Carbohydr. Res.* **1992**, *233*, 15–34.
7. Dowd, M. K.; French, A. D.; Reilly, P. J. *J. Carbohydr. Chem.* **1995**, *14*, 589–600.
8. Mendonca, S.; Johnson, G. P.; French, A. D.; Laine, R. A. *J. Phys. Chem. A* **2002**, *106*, 4115–4124.
9. Allinger, N. L.; Yuh, Y. H.; Lii, J.-H. *J. Am. Chem. Soc.* **1989**, *111*, 8551–8566.
10. Allinger, N. L.; Rahman, M.; Lii, J.-H. *J. Am. Chem. Soc.* **1990**, *112*, 8293–8307.
11. Stortz, C. A.; Cerezo, A. S. *Carbohydr. Res.* **2002**, *337*, 1861–1871.
12. Stortz, C. A.; Cerezo, A. S. *Carbohydr. Res.* **2003**, *338*, 95–107.
13. Stortz, C. A.; Cerezo, A. S. *Biopolymers* **2003**, *70*, 227–239.
14. Ponce, N. M. A.; Pujol, C. A.; Damonte, E. B.; Flores, M. L.; Stortz, C. A. *Carbohydr. Res.* **2003**, *338*, 153–165.
15. Ribeiro, A. C.; Vieira, R. P.; Mourão, P. A. S.; Mulloy, B. *Carbohydr. Res.* **1994**, *255*, 225–240.
16. Mulloy, B.; Ribeiro, A. C.; Alves, A. P.; Vieira, R. P.; Mourão, P. A. S. *J. Biol. Chem.* **1994**, *269*, 22113–22123.
17. Bilan, M. I.; Grachev, A. A.; Ustuzhanina, N. E.; Shashkov, A. S.; Nifantiev, N. E.; Usov, A. I. *Carbohydr. Res.* **2004**, *339*, 511–517.
18. Khatuntseva, E. A.; Ustuzhanina, N. E.; Zatonskii, G. V.; Shashkov, A. S.; Usov, A. I.; Nifant'ev, N. E. *J. Carbohydr. Chem.* **2000**, *19*, 1151–1173.
19. Gerbst, A. G.; Ustuzhanina, N. E.; Grachev, A. A.; Zlotina, N. S.; Khatuntseva, E. A.; Tsvetkov, D. E.; Shashkov, A. S.; Usov, A. I.; Nifantiev, N. E. *J. Carbohydr. Chem.* **2002**, *21*, 313–324.
20. Gerbst, A. G.; Ustuzhanina, N. E.; Grachev, A. A.; Khatuntseva, E. A.; Tsvetkov, D. E.; Shashkov, A. S.; Usov, A. I.; Preobrazhenskaya, M. E.; Ushakova, N. A.; Nifantiev, N. E. *J. Carbohydr. Chem.* **2003**, *22*, 109–122.
21. MM3 (96) *Bull. QCPE* **1997**, *17*(1), 3.
22. Lamba, D.; Glover, S.; Mackie, W.; Rashid, A.; Sheldrick, B.; Pérez, S. *Glycobiology* **1994**, *4*, 151–163.
23. Engelsen, S. B.; Koča, J.; Braccini, I.; Hervé du Penhoat, C.; Pérez, S. *Carbohydr. Res.* **1995**, *276*, 1–29.
24. Imberty, A.; Tran, V.; Pérez, S. *J. Comput. Chem.* **1989**, *11*, 205–216.
25. Schirmer, R. E.; Noggle, J. H.; Davis, J. P.; Hart, P. A. *J. Am. Chem. Soc.* **1970**, *92*, 3266–3273.
26. Stortz, C. A.; Cerezo, A. S. *J. Carbohydr. Chem.* **1998**, *17*, 1405–1419.
27. Stortz, C. A. *Carbohydr. Res.* **2002**, *337*, 2311–2323.
28. Koča, J.; Pérez, S.; Imberty, A. *J. Comput. Chem.* **1995**, *16*, 296–310.
29. Luger, P.; Vangehr, K.; Bock, K.; Paulsen, H. *Carbohydr. Res.* **1983**, *117*, 23–38.
30. Stortz, C. A.; Cerezo, A. S. *J. Carbohydr. Chem.* **2002**, *21*, 355–371.
31. Stortz, C. A.; Cerezo, A. S. *J. Carbohydr. Chem.* **2003**, *22*, 217–239.